HHS Public Access

Author manuscript

Clin Neurophysiol. Author manuscript; available in PMC 2017 June 01.

Published in final edited form as:

Clin Neurophysiol. 2016 June ; 127(6): 2489–2499. doi:10.1016/j.clinph.2016.03.022.

Interictal high-frequency oscillations generated by seizure onset and eloquent areas may be differentially coupled with different slow waves

Yutaka Nonoda, MD[1], **Makoto Miyakoshi, PhD**[4], **Alejandro Ojeda, PhD**[4], **Scott Makeig, PhD**[4], **Csaba Juhász, MD, PhD**[1,2], **Sandeep Sood, MD**[3], and **Eishi Asano, MD, PhD**[1,2,*]

[1]Pediatrics, Children's Hospital of Michigan, Wayne State University, Detroit, MI, USA

[2]Neurology, Children's Hospital of Michigan, Wayne State University, Detroit, MI, USA

[3]Neurosurgery, Children's Hospital of Michigan, Wayne State University, Detroit, MI, USA

[4]Swartz Center for Computational Neuroscience, Institute for Neural Computation, University of California San Diego, La Jolla, CA, USA

Abstract

OBJECTIVE—High-frequency oscillations (HFOs) can be spontaneously generated by seizure-onset and functionally-important areas. We determined if consideration of the spectral frequency bands of coupled slow-waves could distinguish between epileptogenic and physiological HFOs.

METHODS—We studied a consecutive series of 13 children with focal epilepsy who underwent extraoperative electrocorticography. We measured the occurrence rate of HFOs during slow-wave sleep at each electrode site. We subsequently determined the performance of HFO rate for localization of seizure-onset sites and undesirable detection of nonepileptic sensorimotor-visual sites defined by neurostimulation. We likewise determined the predictive performance of modulation index: $MI_{(XHz)\&(YHz)}$, reflecting the strength of coupling between amplitude of $HFOs_{XHz}$ and phase of $slow\text{-}wave_{YHz}$. The predictive accuracy was quantified using the area under the curve (AUC) on receiver-operating characteristics analysis.

RESULTS—Increase in HFO rate localized seizure-onset sites (AUC≥0.72; p<0.001), but also undesirably detected nonepileptic sensorimotor-visual sites (AUC≥0.58; p<0.001). Increase in $MI_{(HFOs)\&(3–4Hz)}$ also detected both seizure-onset (AUC≥0.74; p<0.001) and nonepileptic sensorimotor-visual sites (AUC≥0.59; p<0.001). Increase in subtraction-MI_{HFOs} [defined as subtraction of $MI_{(HFOs)\&(0.5–1Hz)}$ from $MI_{(HFOs)\&(3–4Hz)}$] localized seizure-onset sites

*Corresponding Author: Eishi Asano, MD, PhD, MS (CRDSA), Division of Pediatric Neurology, Children's Hospital of Michigan, Wayne State University. 3901, Beaubien St., Detroit, MI, 48201, USA, Tel.: +1-313-745-5547, Fax: +1-313-745-0955, eishi@pet.wayne.edu.

CONFLICT OF INTEREST

None of the authors have potential conflicts of interest to be disclosed.

(AUC≥0.71; p<0.001), but rather avoided detection of nonepileptic sensorimotor-visual sites (AUC≤0.42; p<0.001).

CONCLUSION—Our data suggest that epileptogenic HFOs may be coupled with slow-wave$_{3–4Hz}$ more preferentially than slow-wave$_{0.5–1Hz}$, whereas physiologic HFOs with slow-wave$_{0.5–1Hz}$ more preferentially than slow-wave$_{3–4Hz}$ during slow-wave sleep.

SIGNIFICANCE—Further studies in larger samples are warranted to determine if consideration of the spectral frequency bands of slow-waves coupled with HFOs can positively contribute to presurgical evaluation of patients with focal epilepsy.

Keywords

High-frequency oscillations (HFOs); Ripples; High-gamma activity; Neurophysiology; Subdural electroencephalography (EEG); Intracranial electrocorticography (ECoG) recording; Pediatric epilepsy surgery; EEGLAB; Phase-amplitude coupling; Subtraction modulation index co-registered to MRI (SMICOM); Receiver-operating characteristics (ROC) curve

INTRODUCTION

Extraoperative electrocorticography (ECoG) is commonly utilized as a part of presurgical evaluation for patients with medically-uncontrolled focal seizures in a number of epilepsy centers. The ultimate purpose of extraoperative ECoG is localization of the epileptogenic zone of which surgical resection results in seizure control as well as delineation of the eloquent areas of which preservation minimizes the risk of postoperative functional deficits (Rosenow and Lüders, 2001). The gold-standard electrophysiological biomarkers for estimation of the epileptogenic zone include the seizure-onset zone involved in generation of habitual seizures, namely, the electrode site(s) initially showing the ictal ECoG discharges prior to habitual seizures (Asano et al., 2009). Conversely, significance of seizure-onset zones involved in non-habitual seizures is currently unknown (Kovac et al., 2014). A long period of extraoperative ECoG recording may be undesirably needed to capture habitual seizures, and some patients do not achieve seizure-freedom even after complete resection of the seizure-onset zone (Asano et al., 2009). Thus, investigators are currently looking for alternative biomarkers estimating the extent of the epileptogenic zone.

Promising candidate biomarkers include interictal high-frequency oscillations (HFOs) spontaneously and intermittently generated during resting periods (Jacobs et al., 2012; Zijlmans et al., 2012). Studies of both pediatric and adult populations reported that surgical failure was associated with a high rate of interictal HFOs generated by the non-resected tissues during non-REM sleep and under general anesthesia (Jacobs et al., 2010; Wu et al., 2010; Akiyama et al., 2011; van't Klooster et al., 2015). A large number of investigators independently reported that electrode sites frequently generating HFOs often turn out to be a part of the seizure-onset zones (Staba et al., 2002; Bagshaw et al., 2009; Crépon et al., 2010; Akiyama et al., 2011; Blanco et al., 2011; Gliske et al., 2015; Sakuraba et al., 2015). Sites showing HFOs$_{>80Hz}$ and HFOs$_{>250Hz}$ are often overlapped in space (Jacobs et al., 2011), but HFOs$_{>80Hz}$ are generated by larger brain regions (Zijlmans et al., 2012). Some studies suggested that the occurrence rate of HFOs$_{>250Hz}$ predicted the postoperative seizure outcome somewhat better than that of HFOs$_{>80Hz}$ (Akiyama et al., 2011; van't Klooster et

al., 2015). Others suggested that $HFOs_{>80Hz}$ may be more useful than $HFOs_{>250Hz}$, which are difficult to detect in a substantial proportion of patients with neocortical epilepsy (Blanco et al., 2011; Wang et al., 2013).

Despite the efforts of many investigators, the clinical utility of interictal HFOs still remains uncertain (Jobst, 2013), particularly because HFOs are frequently generated by nonepileptic visual, somatosensory, motor, and auditory cortices during resting periods (Blanco et al., 2011; Fukushima et al., 2012; Nagasawa et al., 2012; Melani et al., 2013; Wang et al., 2013; Alkawadri et al., 2014; van't Klooster et al., 2015). The current recommendation is that one should not determine the resection margin solely based on the occurrence rate or spectral frequency band of interictal HFOs (Engel et al., 2009; Asano et al., 2013; Gliske et al., 2015). A method that can distinguish epileptogenic from physiologic HFOs in an automatic and efficient manner is highly desirable.

Our central hypothesis was that consideration of the spectral frequency band of slow-waves coupled with HFOs would improve the specificity of prediction of seizure-onset zone responsible for generation of habitual seizures. Our preliminary study of interictal ECoG during slow-wave sleep showed that HFOs in the nonepileptic occipital pole were strictly coupled with slow wave at 1 Hz and below, whereas HFOs in the seizure-onset zones coupled with slow wave at 3–4 Hz also (Nagasawa et al., 2012). Another group reported that both nonepileptic visual and sensorimotor areas can frequently generate interictal HFOs independent from interictal spike discharges (Wang et al., 2013). It is plausible that seizure-onset zone could be predicted by measuring *in situ* modulation index: $MI_{(HFOs)\&(slow\text{-}wave)}$, a measure that reflects the degree of stability of phase-amplitude coupling between HFO amplitude and slow-wave phase (Canolty et al., 2006). In theory, $MI_{(>XHz)\&(YHz)}$ is greater if a larger amplitude of $HFOs_{>XHz}$ are more consistently coupled with a phase of $slow\text{-}wave_{YHz}$. Here, we measured MI at all electrode sites during interictal state on the first evening of extraoperative ECoG recording, using an open source toolbox EEGLAB and its extension Phase-Amplitude Coupling Toolbox (PACT) that incorporates the algorithm and routines for measurement of MI (Miyakoshi et al., 2013).

The first aim of this study was to determine, using receiver operating characteristics (ROC) analysis, how accurately the rates of $HFOs_{>80Hz}$, $HFOs_{>150Hz}$, and $HFOs_{>250Hz}$ predicted the seizure-onset sites. The next aim was to determine how accurately, but undesirably, the rates of these HFO rates detected the nonepileptic sensorimotor-visual sites clinically defined by neurostimulation. We subsequently measured $MI_{(HFOs)\&(3–4Hz)}$ and $MI_{(HFOs)\&(0.5–1Hz)}$ at all electrode sites, and determined how accurately the seizure-onset and nonepileptic sensorimotor-visual sites were detected by $MI_{(HFOs)\&(3–4Hz)}$ and $MI_{(HFOs)\&(0.5–1Hz)}$, respectively. According to the results of previous studies (Nagasawa et al., 2012; Wang et al., 2013), we expected that seizure-onset sites would be associated with increased $MI_{(HFOs)\&(3–4Hz)}$ and that nonepileptic sensorimotor-visual sites would be associated with increased $MI_{(HFOs)\&(0.5–1Hz)}$. Specifically, we tested the hypothesis that subtraction-MI_{HFOs} [defined as subtraction of $MI_{(HFOs)\&(0.5–1Hz)}$ from $MI_{(HFOs)\&(3–4Hz)}$] would localize the seizure-onset sites with reduced detection of the nonepileptic sensorimotor-visual sites.

METHODS

Patients

The inclusion criteria consisted of: (i) a two-stage epilepsy surgery using extraoperative subdural ECoG recording in Children's Hospital of Michigan, Detroit, between October 2013 and September 2014, (ii) ECoG sampling from all four lobes of the affected hemisphere, and (iii) habitual seizures captured during extraoperative ECoG recording. The exclusion criteria consisted of (i) presence of massive brain malformations, such as large porencephaly, perisylvian polymicrogyria, or hemimegalencephaly, which are known to confound the anatomical landmarks for the central, calcarine, and sylvian sulci, (ii) undergoing hemispherectomy, and (iii) age of six years and younger (Haseeb et al., 2007). We studied a consecutive series of 13 children with a diagnosis of medically-uncontrolled focal epilepsy (age range: 7.9 – 18.8 years; 10 females; Table 1) who satisfied the inclusion and exclusion criteria. The study has been approved by the Institutional Review Board at Wayne State University, and written informed consent was obtained from the guardians of all patients.

Subdural electrode placement

Platinum macro-electrodes (inter-contact distance: 10 mm; contacts: 104 to 144 per patient) were placed in the subdural space generously over the affected hemisphere (Supplementary Figures S1–S3), to satisfactorily determine the boundaries between the epileptogenic zone and eloquent areas (Nariai et al., 2011; Nagasawa et al., 2012). Our standardized placement of subdural electrodes included strip electrodes over the medial and inferior surfaces of temporal and occipital lobes, an 8-by-8 grid electrode array over the lateral temporal-frontal-parietal surface including the pre- and post-central gyri. Additional strip electrodes were placed on the inferior surface of the frontal lobe as well as the medial surface of the frontal-parietal region, based on the results of non-invasive presurgical evaluation using scalp video-EEG, MRI and glucose-metabolism positron emission tomography (PET). Such widespread cortical coverage has been commonly practiced, since suboptimal sampling is a major factor of failed surgery (Widdess-Walsh et al., 2007; Kim et al., 2010; Akiyama et al., 2011; Gerrard et al., 2012; Englot et al., 2014). All electrode plates were stitched to adjacent plates or the edge of dura mater to avoid movement of subdural electrodes after placement. The electrode leads were tunneled about an inch from the main wound to minimize the risk of infection. Intraoperative photographs were taken with a digital camera before dural closure. The dura was closed in a semi-watertight fashion and the bone flap was re-placed but not secured. A sub-galeal drain was placed to minimize post-operative scalp swelling. Intracranial pressure monitor was placed, to readily detect intracranial hematoma or excessive brain swelling and to treat it accordingly. It should be noted that we do not place electrodes more than clinically indicated. Patients with a restricted MRI-visible structural lesion (for example, hippocampal sclerosis or brain tumor) do not undergo widespread electrode coverage in our hospital, as long as the epileptogenic zone is estimated to be confined to the lesion using the aforementioned non-invasive diagnostic tools. A three-dimensional surface image was created with the location of electrodes directly defined on the brain surface (Alkonyi et al., 2009; Matsuzaki et al., 2015). For better appreciation of the spatial characteristics, HFO rate (the number of events of interictal HFOs per minute) and

MI measures at a given electrode site were presented on each individual's brain surface image, as previously performed using FreeSurfer (Desikan et al., 2006; Dykstra et al., 2012; Pieters et al., 2013; Matsuzaki et al., 2015).

Extraoperative ECoG recording

ECoG signals were obtained for 3 to 5 days with a sampling rate at 1,000 Hz and an amplifier band pass at 0.016 – 300 Hz, using a 192-channel Nihon Kohden Neurofax 1100A Digital System (Nihon Kohden America Inc, Foothill Ranch, CA, USA). This band pass is supposed to reduce the amplitude of $HFOs_{300Hz}$ by 30% but not necessarily eliminate it. Previous studies of neocortical epilepsy, in which ECoG signals were sampled with macro-electrodes and with a sampling rate at 2,000 Hz suggested that the spectral frequency of interictal HFOs ranged mostly below 300 Hz (Worrell et al., 2008; Wu et al., 2010; Wang et al., 2013).

The averaged voltage of signals derived from the fifth and sixth intracranial electrodes of the amplifier was used as the original reference; signals were then re-montaged to a common average reference (Crone et al., 2001; Canolty et al., 2006; Nagasawa et al., 2012; Sakuraba et al., 2015). Channels contaminated with large interictal epileptiform discharges or artifacts were visually identified and excluded from the common average reference (Fukuda et al., 2008; Zijlmans et al., 2012). No notch filter was used for further analysis in any patients. As a part of routine clinical procedures, surface electromyography electrodes were placed on the left and right deltoid muscles (Nariai et al., 2011). Electrooculography electrodes were placed 2.5 cm below and 2.5 cm lateral to the left and right outer canthi (Nagasawa et al., 2012). Antiepileptic medications were discontinued in the morning prior to subdural electrode placement. Seizure-onset sites, defined as electrode site(s) initially showing sustaining rhythmic ECoG changes prior to the onset of habitual seizures, were visually determined (Asano et al., 2009). Ictal ECoG patterns of epileptic spasms are characterized by fast wave discharges (>30 Hz) quickly propagated to widespread regions (Nariai et al., 2011), whereas those of focal seizures are characterized by either repetitive spike-wave discharges or focal fast wave discharges followed by gradual propagation to the surrounding areas (Asano et al., 2009).

Neurostimulation mapping

Functional cortical mapping by neurostimulation was performed, as a part of routine presurgical evaluation (Supplementary Table S1). The methodological details are available in Haseeb et al., 2007 as well as Kumar et al., 2012. In short, a pulse-train of repetitive electrical stimuli was delivered to neighboring electrode pairs, with stimulus frequency of 50 Hz, pulse duration of 300 μsec, and train duration ranging up to 5 s. Initially, stimulus intensity was set to 3 mA, and stimulus intensity was increased up to 9 mA in a stepwise manner until a clinical response or after-discharge was observed. We determined sensorimotor-visual sites at which stimulation reproducibly resulted in somatosensory or visual perceptual changes or movement of a body part.

Resection of the presumed epileptogenic zone

Resective surgery was tailored to the presumed epileptogenic zone, consisting of (i) seizure-onset sites involved in habitual seizures, (ii) frequent spiking sites not accounted for by propagation from the seizure-onset sites, and (iii) neuroimaging abnormalities surrounding the seizure-onset sites. Thereby, we intended to preserve the eloquent areas defined by neurostimulation mapping as well as their associated vascular structures (Asano et al., 2009). In case the presumed epileptogenic zone overlapped with the eloquent areas, resection margin was determined, on a case-by-case basis, after intense discussion with the family of a given patient regarding the pros and cons of complete resection of the presumed epileptogenic zone.

Measurement of the occurrence rate of interictal high-frequency oscillations (HFOs)

This is a retrospective study, and the results of the following ECoG analyses did not influence the surgical decision. Data were analyzed offline using $EEGLAB_{v.13.4.4b}$ and $PACT_{v.0.17}$ (Delorme and Makeig, 2004; Miyakoshi et al., 2013). The rates of HFOs were measured using the method similar to those reported previously (Jacobs et al., 2010; Wu et al., 2010; Nagasawa et al., 2012; Figure 1). First, a 10-min epoch showing slow-wave sleep (Bagshaw et al., 2009) and at least two hours apart from an ictal event (Worrell et al., 2008) was selected from the ECoG segment with a least amount of artifacts during the first evening after the subdural electrode placement. ECoG signals were visually assessed with a sensitivity of about 10 μV/mm and a display of 2 s/page. On the EEGLAB platform, the signal sensitivity varies according to the default screen-wise normalization for display and user-defined scaling factor. Each $HFOs_{>f\ Hz}$ event was defined as an oscillatory event of ≥6 cycles (Worrell et al., 2008) with a frequency of ≥f Hz, a duration of <400 ms, an amplitude at least five times larger relative to the immediately-preceding baseline. A high-pass filter of 80, 150, and 250 Hz (Kaiser-windowed sinc FIR filter; Kaiser beta: 3.4; filter order: ≤16; Supplementary Figures S4–S6) was applied to ECoG signals in order to visually mark each event of $HFOs_{>80Hz}$, $HFOs_{>150Hz}$, and $HFOs_{>250Hz}$. Visual marking of HFOs was performed by a pediatric neurologist (Y.N.), who was blinded to the locations of seizure-onset sites, those of resection margins, and post-operative seizure outcomes. Since such visual marking is enormously time-consuming (Zijlmans et al., 2009), we could not assign this procedure to another investigator. A 5-min epoch, instead of 10-min, was analyzed in three patients (#4, 5, and 13) whose ECoG showed an extremely high rate of HFOs. Artifactual channels (Otsubo et al., 2008; Nagasawa et al., 2012) were prospectively determined by a board-certified clinical neurophysiologist (E.A.) and excluded from further analysis.

ROC analysis was performed using a method similar to those previously described by other investigators (Figures 2 and 3; Jacobs et al., 2008; Andrade-Valença et al., 2012). First, we combined each predictor measure (e.g.: rate of $HFOs_{>80Hz}$) of all channels derived from 13 patients into a single pool. We delineated an ROC curve for each predictor, and determined how accurately the rates of $HFOs_{>80Hz}$, $HFOs_{>150Hz}$, and $HFOs_{>250Hz}$ localized the seizure-onset sites, according to the generally-accepted notion that the rate of HFOs should be larger in the seizure-onset compared to the other sites (Jacobs et al., 2012; Zijlmans et al., 2012). The performance of each predictor measure for localizing the seizure-onset sites was

quantified by the area under the curve (AUC) of a given ROC curve; namely, an AUC of 1 was considered to be a perfect test, whereas an AUC of 0.5 to be a test no better than random prediction. With a given cut-off threshold common to a group of 13 patients, each ROC curve can provide the sensitivity and specificity of each predictor for localization of seizure-onset sites. Likewise, ROC analysis was applied to determine how accurately, but undesirably, the rates of $HFOs_{>80Hz}$, $HFOs_{>150Hz}$, and $HFOs_{>250Hz}$ detected the nonepileptic sensorimotor-visual sites (defined as sensorimotor-visual sites not classified as the seizure onset). Logistic regression analyses finally determined how much 'each 1/min greater rate of HFOs' indeed increased the odds of a given site to be classified as the seizure-onset (or nonepileptic sensorimotor-visual area). SPSS Statistics 22 (IBM Corp, Chicago, IL, USA) was utilized for statistical analysis. A p-value of 0.05 was taken as statistically significant.

Measurement of modulation index (MI)

MI was calculated in an automatic fashion at each electrode site using the algorithm identical to that previously reported (Miyakoshi et al., 2013). In short, to calculate MI, ECoG signals were high-pass filtered at the frequency of interest (e.g.: 80 Hz). The data were Hilbert transformed and the data points whose instantaneous amplitude fell within the top five percentile of the distribution were defined as HFO and used for computing the strength of coupling with the instantaneous phase of local slow wave of interest (for example, 3–4 Hz). The EEGLAB Toolbox $PACT_{v.0.17}$ can provide: (i) MI value, reflecting the strength of phase-amplitude coupling at a given site, (ii) 95% confidence interval (95%CI) of MI to determine if the strength of phase-amplitude coupling was above the chance level, and (iii) phase angle of slow wave most tightly coupled with given HFO. In the present study, we used an MI value at a given site for localization of seizure-onset sites.

ROC curves determined how well $MI_{(HFOs)\&(3–4Hz)}$ and $MI_{(HFOs)\&(0.5–1Hz)}$ localized the seizure-onset and nonepileptic sensorimotor-visual sites, independently. Subsequently, another ROC analysis determined the prediction performance of subtraction-MI_{HFOs} [defined as subtraction of $MI_{(HFOs)\&(0.5–1Hz)}$ from $MI_{(HFOs)\&(3–4Hz)}$]. Finally, logistic regression analyses determined how much 'each increase of MI measure of interest' indeed increased the odds of a given site to be classified as seizure-onset (or nonepileptic sensorimotor-visual area).

RESULTS

Patient profile

A cortical lesion was appreciated on MRI in four patients (Table 1). The remaining nine patients had normal or nonspecific MRI findings, whereas focal or lateralized glucose hypometabolism was noted on PET in all patients. Extraoperative ECoG recording showed that the median number of seizure-onset electrode sites was 10 (range: 1 to 36; Supplementary Table S1). Neurostimulation mapping localized both somatosensory, motor, and visual sites in all 13 patients (Supplementary Figure S2). Neurostimulation failed to induce auditory hallucination in any of our patients, possibly because electrodes were not placed exactly on the planum temporale in our patient cohort.

Surgical resection involved a single lobe in eight patients, and multiple lobes in five patients (Supplementary Figure S3). The post-operative follow-up period was relatively short in our cohort (median: 19 months). Nine patients achieved seizure freedom following the first surgery (Table 1).

Prediction performance of the rate of HFOs

We have provided the descriptive statistics of HFO rates in Supplementary Table S2. The spatial distributions of occurrence rates were very similar among $HFOs_{>80Hz}$, $HFOs_{>150Hz}$, and $HFOs_{>250Hz}$ (mean Kendall's W across patients: 0.52; p=0.001). Our observations of a smaller rate of $HFOs_{>250Hz}$ compared to that of $HFOs_{>80Hz}$ as well as similar spatial distribution of HFO rates across different spectral frequencies were consistent with those reported in previous studies (Akiyama et al., 2011; Jacobs et al., 2011).

Seizure-onset sites showed greater occurrence rates of HFOs compared to non-seizure-onset sites ($p<0.001$; Table 2). The AUCs of ROC analysis for prediction of the seizure-onset sites using $HFOs_{>80Hz,}$ $HFOs_{>150Hz}$, and $HFOs_{>250Hz}$ were all 0.72. With a sensitivity of 0.50, the specificity of $HFOs_{>80Hz}$, $HFOs_{>150Hz}$, and $HFOs_{>250Hz}$ for prediction of the seizure-onset sites was 0.89, 0.88, and 0.88, respectively. Logistic regression analysis also demonstrated that 'each 1/min increase of HFO rate' indeed increased the odds of a given site to be classified as seizure-onset (Table 3). Difference in seizure-onset localization performance between $HFOs_{>80Hz}$, $HFOs_{>150Hz}$, and $HFOs_{>250Hz}$ was modest.

Nonepileptic sensorimotor-visual sites showed greater rates of HFOs compared to non-sensorimotor-visual sites ($p<0.001$; Table 4). The AUC of ROC analysis for undesirable detection of nonepileptic sensorimotor-visual sites was 0.60 for $HFOs_{>80Hz}$, 0.62 for $HFOs_{>150Hz}$, and 0.58 for $HFOs_{>250Hz}$. With a sensitivity of 0.50, the specificity of $HFOs_{>80Hz}$, $HFOs_{>150Hz}$, and $HFOs_{>250Hz}$ for undesirable detection of the nonepileptic sensorimotor-visual sites was 0.66, 0.67, and 0.67, respectively. Logistic regression analysis failed to show that 'each 1/min increase of HFO rate' increased the odds of a given site to be classified as a nonepileptic sensorimotor-visual site with statistical significance (Table 5).

Prediction performance of modulation index (MI)

We found that the calculation time of MI was less than three minutes per patient. We have provided the descriptive statistics of MI measures in Supplementary Table S2. The spatial distributions of $MI_{(HFOs)\&(0.5–1Hz)}$ and $MI_{(HFOs)\&(3–4Hz)}$ were similar but not identical (mean Spearman's rho across patients: ≥0.64; p=0.001).

$MI_{(HFOs)\&(0.5–1Hz)}$, $MI_{(HFOs)\&(3–4Hz)}$, and subtraction-MI_{HFOs} in the seizure-onset sites were larger compared to those in the non-seizure-onset sites ($p\leq0.001$; Table 2). The AUC of ROC analysis for localization of the seizure-onset sites was ≥0.58 for $MI_{(HFOs)\&(0.5–1Hz)}$, ≥0.74 for $MI_{(HFOs)\&(3–4Hz)}$, and ≥0.71 for subtraction-MI_{HFOs}. With a sensitivity of 0.50, the specificity of $MI_{(HFOs)\&(0.5–1Hz)}$, $MI_{(HFOs)\&(3–4Hz)}$, and subtraction-MI_{HFOs} for localization of the seizure-onset sites was ≥0.55, ≥0.88, and ≥0.88, respectively. Logistic regression analysis also demonstrated that greater values of the aforementioned MI measures indeed increased the odds of a given site to be classified as seizure-onset (Table 3).

Nonepileptic sensorimotor-visual sites showed larger $MI_{(HFOs)\&(0.5–1Hz)}$ and smaller subtraction-MI_{HFOs} (Figure 4), compared to non-sensorimotor-visual sites ($p<0.001$; Table 4). The AUC of ROC analysis for undesirable detection of nonepileptic sensorimotor-visual sites was ≥0.60 for $MI_{(HFOs)\&(0.5–1Hz)}$, ≥0.59 for $MI_{(HFOs)\&(3–4Hz)}$, but ≤0.42 for subtraction-MI_{HFOs}. With a sensitivity of 0.50, the specificity of $MI_{(HFOs)\&(0.5–1Hz)}$, $MI_{(HFOs)\&(3–4Hz)}$, and subtraction-MI_{HFOs} was ≥0.63, ≥0.63, and ≤0.36, respectively. Logistic regression analysis suggested that greater $MI_{(>150Hz)\&(0.5–1Hz)}$, $MI_{(>250Hz)\&(0.5–1Hz)}$, and $MI_{(>250Hz)\&(3–4Hz)}$ significantly increased the odds, but greater values of subtraction-MI_{HFOs} rather decreased the odds of a given electrode site to be classified as a nonepileptic sensorimotor-visual site (Table 5).

Post-hoc evaluation of our ECoG analyses and results

After the aforementioned results became available, we determined how similar spatial distributions were shared by the rate of HFOs and MI. The rate of HFOs was highly correlated with $MI_{(HFOs)\&(3–4Hz)}$ (mean rho across patients: 0.70 for $HFOs_{>80Hz}$, 0.68 for $HFOs_{>150\ Hz}$, and 0.56 for $HFOs_{>250\ Hz}$; $p=0.001$) and moderately with $MI_{(HFOs)\&(0.5–1Hz)}$ (mean rho: 0.60 for $HFOs_{>80Hz}$, 0.56 for $HFOs_{>150\ Hz}$, and 0.43 for $HFOs_{>250\ Hz}$; $p=0.001$). This finding suggests that time-consuming visual marking of HFO events by a single investigator was highly correlated to an electrophysiological index precisely and swiftly generated by a software package. In addition, this finding suggests that $MI_{(HFOs)\&(3–4Hz)}$, compared to $MI_{(HFOs)\&(0.5–1Hz)}$, might better serve as a biomarker with a diagnostic utility similar to that of rate of HFOs.

Post-hoc evaluation revealed that both nonepileptic sensorimotor and visual sites shared similar but not identical HFOs and MI profiles. HFOs in nonepileptic visual sites were strongly coupled with slow wave at 0.5–1 Hz relatively to 3–4 Hz, while the effect size of such phase-amplitude coupling was modest in nonepileptic sensorimotor sites. For example, the AUC of ROC analysis for undesirable detection of nonepileptic visual sites was 0.75 for rate of $HFOs_{>150Hz}$, 0.80 for $MI_{(>150Hz)\&(0.5–1Hz)}$, 0.77 for $MI_{(>150Hz)\&(3–4Hz)}$, and 0.36 for subtraction-$MI_{>150Hz}$ (Supplementary Table S5). Likewise, the AUC for undesirable detection of nonepileptic sensorimotor sites was 0.53 for rate of $HFOs_{>150Hz}$, 0.57 for $MI_{(>150Hz)\&(0.5–1Hz)}$, 0.58 for $MI_{(>150Hz)\&(3–4Hz)}$, and 0.44 for subtraction-$MI_{>150Hz}$ (Supplementary Table S6).

DISCUSSION

Clinical implications

The present study demonstrated that HFOs are commonly generated by both ‘seizure-onset sites determined by extraoperative ECoG recording’ and ‘nonepileptic sensorimotor-visual sites defined by neurostimulation mapping’. The novel findings include that the spatial distribution of rate of HFOs was similar to those of $MI_{(HFOs)\&(3–4Hz)}$ and $MI_{(HFOs)\&(0.5–1Hz)}$. $MI_{(HFOs)\&(3–4Hz)}$ localized the seizure-onset sites with a comparable accuracy with the occurrence rate of HFOs and with a better accuracy than $MI_{(HFOs)\&(0.5–1Hz)}$. While $MI_{(HFOs)\&(3–4Hz)}$ still detected both seizure-onset and nonepileptic sensorimotor-visual sites, subtraction-MI_{HFOs} [defined as subtraction of

$MI_{(HFOs)\&(0.5–1Hz)}$ from $MI_{(HFOs)\&(3–4Hz)}$] reasonably localized seizure-onset sites with reduced detection of nonepileptic sensorimotor-visual sites. The aforementioned observations provide the clinical implications that epileptogenic HFOs may be more preferentially coupled with slow waves of 3–4 Hz, whereas physiological HFOs in the primary visual and sensorimotor cortex may be coupled with those of 0.5–1 Hz during slow-wave sleep. It is too optimistic to expect that subtraction-MI_{HFOs} measures can completely avoid the unwanted detection of nonepileptic sensorimotor-visual sites. Thus, we cannot make a conclusion that the surgical resection can be guided by subtraction-MI_{HFOs} measures alone. We do not suggest that our technique can localize the epileptogenic zone by extracting signal profiles invisible by naked eyes. Rather, the roles of MI measures would include precise and swift quantification of the degree and extent of visible epileptiform discharges during interictal state. Further studies of a larger patient cohort are needed to determine if interictal MI measures can be clinically utilized as a supplementary tool to estimate the epileptogenic zone. We are also willing to share our technique and dataset to facilitate the external validation and improvement of the analytical approaches utilized in this study.

The plausible explanations for the successful localization of seizure-onset sites by $MI_{(HFOs)\&(3–4Hz)}$ include that interictal spike discharges, frequently coupled with slow-wave of 3–4 Hz, often arise from the seizure-onset zone in patients with focal epilepsy (Hufnagel et al., 2000; Asano et al., 2003). It is likely that a high value of $MI_{(HFOs)\&(3–4Hz)}$ at a given site was attributed to the large amplitude of spike discharges, since the spike component contains high-frequency activity widely involving >80 Hz (Jacobs et al., 2011; Usui et al., 2015). Spike discharges are typically coupled with slow waves of 3–3.5 Hz in absence epilepsy and 3–4 Hz in juvenile myoclonic epilepsy as well as focal epilepsy (Moeller et al., 2008; Berg and Scheffer, 2011; Nagasawa et al., 2012). The mechanism defining the spectral frequency band of slow waves following spike discharges remains unknown. A study of ferret brain slices demonstrated that a single pulse stimulus (mimicking normal action potential firing) of the cortico-thalamic tract resulted in 6–10Hz oscillations resembling sleep spindles, whereas repetitive train stimuli at 200 Hz resulted in 3–4 Hz oscillations resembling absence seizures (Blumenfeld and McCormick, 2000). Studies of human cerebral cortex also reported that a single pulse cortical stimulation of seizure-onset sites induces spike-and-slow-wave discharges in the surrounding regions, where the spectral frequency of induced slow-waves often ranges from 3–4 Hz (van't Klooster et al., 2011; Nayak et al., 2014; Mouthaan et al., 2015). An ECoG study of patients with focal epilepsy suggested that increased $MI_{(80–150Hz)\&(1–25Hz)}$ on macro-electrodes during a seizure was associated with strong multi-unit firing bursts recorded on micro-electrodes (Weiss et al., 2013).

A plausible explanation for the association between nonepileptic sensorimotor-visual sites and relative increase in $MI_{(HFOs)\&(0.5–1Hz)}$ is that such physiological HFOs are preferentially coupled with large-scale network oscillations generated by healthy brain structures during slow-wave sleep. It has been suggested that sleep-related sensory perceptual learning involves a highly-localized low-level function in the primary sensory cortex, and that HFOs coupled with local slow waves at 0.5–1 Hz might be involved in such perceptual learning or memory consolidations (Steriade and Timofeev, 2003; Marshall et al., 2006; Sasaki et al.,

2010; Schroeder and Lakatos, 2009). It was suggested that the phase of slow waves at <1 Hz during slow-wave sleep may alter the neuronal excitability at a given site, with HFOs preferentially taking place during an excitatory state also known as *up* state (Steriade et al., 1993; Contreras et al., 1996; Sanchez-Vives et al., 2000; Nagasawa et al., 2012).

Methodological considerations

The spatial profiles of HFO rates in each patient would be affected by how an HFO event is defined by different investigators. For visual marking of HFO events, we defined each HFO event as an oscillatory event of ≥6 cycles (Worrell et al., 2008; Nagasawa et al., 2012) with a duration of <400 ms, and an amplitude at least five times larger relative to an immediately-preceding baseline. We visually marked HFOs with such a short duration only, since some investigators indicated that physiological HFOs might have a long duration (Melani et al., 2013). For computation of MI, the algorithm does not take into account the number of oscillations of each event of HFOs; thus, an oscillatory event of <6 cycles could be treated as HFO as long as the instantaneous amplitude fell within the top five percentile of the distribution at a given site.

We selected a 10-minute epoch from slow-wave sleep in the first evening, regardless of the presence or absence of interictal epileptiform discharges. We cannot rule out the possibility that the rate of interictal epileptiform discharges may drastically alter the spatial profiles of $MI_{(HFOs)\&(3–4Hz)}$. We found that patients #6, 8, and 9 showed no interictal spike-and-wave discharges during the 10-minue epoch. It is possible that another 10-minute epoch during the second or third evening might have shown more abundant interictal spike-and-wave discharges and that MI measures might have resulted in a better accuracy for prediction of seizure-onset sites.

$MI_{(HFOs)\&(3–4Hz)}$ within a same individual but during distinct epochs would be of interest. We expect that higher occurrence rate of interictal spike-and-wave discharges would be correlated with higher $MI_{(HFOs)\&(3–4Hz)}$ at a given site. Recent studies using scalp EEG and ECoG recordings reported that interictal spike-and-wave discharges as well as $HFOs_{>80Hz}$ tend to involve a restricted region close to the seizure-onset zones during REM sleep but more widespread regions during non-REM sleep (Okanari et al., 2015; Sakuraba et al., 2015). Several studies of ictal and pre-ictal ECoG recording reported that $MI_{(HFOs)\&(slow\text{-}wave)}$ can increase in the seizure-onset sites prior to and during seizures (Weiss et al., 2013; Alvarado-Rojas et al., 2014; Ibrahim et al., 2014; Guirgis et al., 2015).

Another factor affecting the prediction performance would be the location of subdural electrode placement, which involved all four lobes in the affected hemisphere in the present study. Our widespread electrode coverage still missed several cortical structures including the planum temporale, frontal-parietal operculum, and insular cortex. Patient #1 enjoyed cessation of habitual epileptic spasms for eight months following the first surgery consisting of temporal-occipital-parietal resection with the post-central gyrus preserved, but focal seizures involving the face and throat emerged afterwards. This patient has been free from both spasms and focal seizures for three months following the second surgery consisting of resection of the parietal operculum and insular cortex not originally sampled in the first

surgery. This case story illustrates the sampling limitation which is inevitably associated with intracranial ECoG recording.

The novel analytical approach in this study includes a correlation between MI measures and nonepileptic sensorimotor-visual sites defined by neurostimulation, the clinical gold-standard for localization of eloquent areas. In the present study, neighboring electrodes were stimulated in a bipolar manner. It was suggested that bipolar and monopolar neurostimulation is equally accurate for identification of eloquent areas (Kombos et al., 1999), whereas bipolar stimulation is less time-consuming and may be more suitable for patients with limited attention span. We cannot exclude the possibility that neurostimulation mapping in the present study could not disclose all nonepileptic sensorimotor-visual sites, since investigators reported that resection of the sites not classified to be eloquent by cortical stimulation can sometimes result in postoperative functional deficits (Kral et al., 2007; Cervenka et al., 2013; Kojima et al., 2013).

In the present study, we analyzed ECoG signals at each site independently from others; thus, we did not take into account the propagation pattern of each HFO event. Further studies are warranted to determine if application of additional multivariate statistics, such as independent component analysis (Bell and Sejnowski, 1995; Onton and Makeig, 2006), would successfully delineate the origin and propagation of HFOs and further improve seizure-onset prediction by interictal ECoG.

Our study was not designed to correlate interictal MI measures and cognitive-related sites defined by either neurostimulation or event-related ECoG changes (e.g.: Kojima et al., 2013). A number of ECoG studies have reported that non-epileptic sites can show increased coupling between ‘HFO amplitude’ and ‘phase of theta/alpha activity’ during tasks requiring memory, language, or attention during awake state (Canolty et al., 2006; Jacobs and Kahana, 2009; Voytek et al., 2010). It has been hypothesized that such slow waves of theta/alpha range coupled with HFOs may play a role in transferring information between distant brain regions (Fell and Axmacher, 2011). Additional studies are needed to characterize $MI_{(HFOs)\&(slow\text{-}wave)}$ in seizure-onset, sensorimotor, visual, and cognitive-related sites during different sleep states. Also, studies using larger samples are needed to determine the following hypotheses on the seizure onset zone involving eloquent areas in the future. Our working hypothesis is that HFOs in sensorimotor-visual areas would be coupled preferentially with slow wave at 3–4 Hz when frequent interictal spikes are present but otherwise coupled with that of 0.5–1 Hz during slow-wave sleep.

Future plan

We plan to determine how well interictal MI measures could contribute to the prediction of long-term post-operative seizure outcome in a larger cohort of patients who underwent epilepsy surgery in our hospital before October 2013. We propose the logistic regression and ROC analyses, as similarly performed in Asano et al., 2009. We also plan to explore how well the seizure outcome was predicted by a model incorporating interictal MI measures but not ictal measures.

Supplementary Material

Refer to Web version on PubMed Central for supplementary material.

Acknowledgments

This work was supported by NIH grants NS64033 (to E. Asano) as well as the intramural grant from Children's Hospital of Michigan Foundation (to E. Asano). We are grateful to Harry T. Chugani, MD, and Carol Pawlak, REEG/EPT at Children's Hospital of Michigan, Wayne State University for the collaboration and assistance in performing the studies described above.

References

Akiyama T, McCoy B, Go CY, Ochi A, Elliott IM, Akiyama M, Donner EJ, Weiss SK, Snead OC 3rd, Rutka JT, Drake JM, Otsubo H. Focal resection of fast ripples on extraoperative intracranial EEG improves seizure outcome in pediatric epilepsy. Epilepsia. 2011; 52:1802–11. [PubMed: 21801168]

Alkawadri R, Gaspard N, Goncharova II, Spencer DD, Gerrard JL, Zaveri H, Duckrow RB, Blumenfeld H, Hirsch LJ. The spatial and signal characteristics of physiologic high frequency oscillations. Epilepsia. 2014; 55:1986–95. [PubMed: 25470216]

Alkonyi B, Juhász C, Muzik O, Asano E, Saporta A, Shah A, Chugani HT. Quantitative brain surface mapping of an electrophysiologic/metabolic mismatch in human neocortical epilepsy. Epilepsy Res. 2009; 87:77–87. [PubMed: 19734012]

Alvarado-Rojas C, Valderrama M, Fouad-Ahmed A, Feldwisch-Drentrup H, Ihle M, Teixeira CA, Sales F, Schulze-Bonhage A, Adam C, Dourado A, Charpier S, Navarro V, Le Van Quyen M. Slow modulations of high-frequency activity (40–140-Hz) discriminate preictal changes in human focal epilepsy. Sci Rep. 2014; 4:4545. [PubMed: 24686330]

Andrade-Valença L, Mari F, Jacobs J, Zijlmans M, Olivier A, Gotman J, Dubeau F. Interictal high frequency oscillations (HFOs) in patients with focal epilepsy and normal MRI. Clin Neurophysiol. 2012; 123:100–5. [PubMed: 21727025]

Asano E, Muzik O, Shah A, Juhász C, Chugani DC, Sood S, Janisse J, Ergun EL, Ahn-Ewing J, Shen C, Gotman J, Chugani HT. Quantitative interictal subdural EEG analyses in children with neocortical epilepsy. Epilepsia. 2003; 44:425–34. [PubMed: 12614399]

Asano E, Juhász C, Shah A, Sood S, Chugani HT. Role of subdural electrocorticography in prediction of long-term seizure outcome in epilepsy surgery. Brain. 2009; 132:1038–47. [PubMed: 19286694]

Asano E, Brown EC, Juhász C. How to establish causality in epilepsy surgery. Brain Dev. 2013; 35:706–20. [PubMed: 23684007]

Bagshaw AP, Jacobs J, LeVan P, Dubeau F, Gotman J. Effect of sleep stage on interictal high-frequency oscillations recorded from depth macroelectrodes in patients with focal epilepsy. Epilepsia. 2009; 50:617–28. [PubMed: 18801037]

Bell AJ, Sejnowski TJ. An information-maximization approach to blind separation and blind deconvolution. Neural Comput. 1995; 7:1129–59. [PubMed: 7584893]

Berg AT, Scheffer IE. New concepts in classification of the epilepsies: entering the 21st century. Epilepsia. 2011; 52:1058–62. [PubMed: 21635233]

Blanco JA, Stead M, Krieger A, Stacey W, Maus D, Marsh E, Viventi J, Lee KH, Marsh R, Litt B, Worrell GA. Data mining neocortical high-frequency oscillations in epilepsy and controls. Brain. 2011; 134:2948–59. [PubMed: 21903727]

Blumenfeld H, McCormick DA. Corticothalamic inputs control the pattern of activity generated in thalamocortical networks. J Neurosci. 2000; 20:5153–62. [PubMed: 10864972]

Canolty RT, Edwards E, Dalal SS, Soltani M, Nagarajan SS, Kirsch HE, Berger MS, Barbaro NM, Knight RT. High gamma power is phase-locked to theta oscillations in human neocortex. Science. 2006; 313:1626–8. [PubMed: 16973878]

Cervenka MC, Corines J, Boatman-Reich DF, Eloyan A, Sheng X, Franaszczuk PJ, Crone NE. Electrocorticographic functional mapping identifies human cortex critical for auditory and visual naming. Neuroimage. 2013; 69:267–76. [PubMed: 23274183]

Chugani HT, Asano E, Juhász C, Kumar A, Kupsky WJ, Sood S. “Subtotal” hemispherectomy in children with intractable focal epilepsy. Epilepsia. 2014; 55:1926–33. [PubMed: 25366422]

Contreras D, Timofeev I, Steriade M. Mechanisms of long-lasting hyperpolarizations underlying slow sleep oscillations in cat corticothalamic networks. J Physiol. 1996; 494:251–64. [PubMed: 8814619]

Crépon B, Navarro V, Hasboun D, Clemenceau S, Martinerie J, Baulac M, Adam C, Le Van Quyen M. Mapping interictal oscillations greater than 200 Hz recorded with intracranial macroelectrodes in human epilepsy. Brain. 2010; 133:33–45. [PubMed: 19920064]

Crone NE, Boatman D, Gordon B, Hao L. Induced electrocorticographic gamma activity during auditory perception. Brazier Award-winning article, 2001. Clin Neurophysiol. 2001; 112:565–82. [PubMed: 11275528]

Delorme A, Makeig S. EEGLAB: an open source toolbox for analysis of single-trial EEG dynamics including independent component analysis. J Neurosci Methods. 2004; 134:9–21. [PubMed: 15102499]

Desikan RS, Ségonne F, Fischl B, Quinn BT, Dickerson BC, Blacker D, Buckner RL, Dale AM, Maguire RP, Hyman BT, Albert MS, Killiany RJ. An automated labeling system for subdividing the human cerebral cortex on MRI scans into gyral based regions of interest. Neuroimage. 2006; 31:968–80. [PubMed: 16530430]

Dykstra AR, Chan AM, Quinn BT, Zepeda R, Keller CJ, Cormier J, Madsen JR, Eskandar EN, Cash SS. Individualized localization and cortical surface-based registration of intracranial electrodes. Neuroimage. 2012; 59:3563–70. [PubMed: 22155045]

Engel J Jr, Bragin A, Staba R, Mody I. High-frequency oscillations: what is normal and what is not? Epilepsia. 2009; 50:598–604. [PubMed: 19055491]

Englot DJ, Raygor KP, Molinaro AM, Garcia PA, Knowlton RC, Auguste KI, Chang EF. Factors associated with failed focal neocortical epilepsy surgery. Neurosurgery. 2014; 75:648–5. [PubMed: 25181435]

Fell J, Axmacher N. The role of phase synchronization in memory processes. Nat Rev Neurosci. 2011; 12:105–18. [PubMed: 21248789]

Fukuda M, Nishida M, Juhász C, Muzik O, Sood S, Chugani HT, Asano E. Short-latency median-nerve somatosensory-evoked potentials and induced gamma-oscillations in humans. Brain. 2008; 131:1793–805. [PubMed: 18508784]

Fukushima M, Saunders RC, Leopold DA, Mishkin M, Averbeck BB. Spontaneous high-gamma band activity reflects functional organization of auditory cortex in the awake macaque. Neuron. 2012; 74:899–910. [PubMed: 22681693]

Gerrard J, Zavari HP, Kasoff WS, Vives KP, Hirsch LR, Duckrow BR, Spencer DD. Expanding the intracranial montage does not increase ICEEG morbidity. Epilepsy Curr. 2012; 13:292.

Gliske SV, Irwin ZT, Davis KA, Sahaya K, Chestek C, Stacey WC. Universal automated high frequency oscillation detector for real-time, long term EEG. Clin Neurophysiol. 201510.1016/j.clinph.2015.07.016

Guirgis M, Chinvarun Y, Del Campo M, Carlen PL, Bardakjian BL. Defining regions of interest using cross-frequency coupling in extratemporal lobe epilepsy patients. J Neural Eng. 2015; 12:026011. [PubMed: 25768723]

Haseeb A, Asano E, Juhász C, Shah A, Sood S, Chugani HT. Young patients with focal seizures may have the primary motor area for the hand in the postcentral gyrus. Epilepsy Res. 2007; 76:131–9. [PubMed: 17723289]

Hufnagel A, Dümpelmann M, Zentner J, Schijns O, Elger CE. Clinical relevance of quantified intracranial interictal spike activity in presurgical evaluation of epilepsy. Epilepsia. 2000; 41:467–78. [PubMed: 10756415]

Ibrahim GM, Wong SM, Anderson RA, Singh-Cadieux G, Akiyama T, Ochi A, Otsubo H, Okanishi T, Valiante TA, Donner E, Rutka JT, Snead OC 3rd, Doesburg SM. Dynamic modulation of epileptic high frequency oscillations by the phase of slower cortical rhythms. Exp Neurol. 2014; 251:30–8. [PubMed: 24211781]

Jacobs J, LeVan P, Chander R, Hall J, Dubeau F, Gotman J. Interictal high-frequency oscillations (80–500 Hz) are an indicator of seizure onset areas independent of spikes in the human epileptic brain. Epilepsia. 2008; 49:1893–907. [PubMed: 18479382]

Jacobs J, Kahana MJ. Neural representations of individual stimuli in humans revealed by gamma-band electrocorticographic activity. J Neurosci. 2009; 29:10203–14. [PubMed: 19692595]

Jacobs J, Zijlmans M, Zelmann R, Chatillon CE, Hall J, Olivier A, Dubeau F, Gotman J. High-frequency electroencephalographic oscillations correlate with outcome of epilepsy surgery. Ann Neurol. 2010; 67:209–20. [PubMed: 20225281]

Jacobs J, Kobayashi K, Gotman J. High-frequency changes during interictal spikes detected by time-frequency analysis. Clin Neurophysiol. 2011; 122:32–42. [PubMed: 20599418]

Jacobs J, Staba R, Asano E, Otsubo H, Wu JY, Zijlmans M, Mohamed I, Kahane P, Dubeau F, Navarro V, Gotman J. High-frequency oscillations (HFOs) in clinical epilepsy. Prog Neurobiol. 2012; 98:302–15. [PubMed: 22480752]

Jobst BC. Are HFOs Still UFOs? The Known and Unknown About High Frequency Oscillations in Epilepsy Surgery. Epilepsy Curr. 2013; 13:273–5. [PubMed: 24348125]

Kim DW, Lee SK, Nam H, Chu K, Chung CK, Lee SY, Choe G, Kim HK. Epilepsy with dual pathology: surgical treatment of cortical dysplasia accompanied by hippocampal sclerosis. Epilepsia. 2010; 51:1429–35. [PubMed: 19919662]

Kojima K, Brown EC, Rothermel R, Carlson A, Fuerst D, Matsuzaki N, Shah A, Atkinson M, Basha M, Mittal S, Sood S, Asano E. Clinical significance and developmental changes of auditory-language-related gamma activity. Clin Neurophysiol. 2013; 124:857–69. [PubMed: 23141882]

Kombos T, Suess O, Kern BC, Funk T, Hoell T, Kopetsch O, Brock M. Comparison between monopolar and bipolar electrical stimulation of the motor cortex. Acta Neurochir. 1999; 141:1295–301. [PubMed: 10672300]

Kovac S, Rodionov R, Chinnasami S, Wehner T, Scott CA, McEvoy AW, Miserocchi A, Diehl B. Clinical significance of nonhabitual seizures during intracranial EEG monitoring. Epilepsia. 2014; 55:e1–5. [PubMed: 24299110]

Kral T, Kurthen M, Schramm J, Urbach H, Meyer B. Stimulation mapping via implanted grid electrodes prior to surgery for gliomas in highly eloquent cortex. Neurosurgery. 2007; 61:319–25. [PubMed: 18813158]

Kumar G, Juhász C, Sood S, Asano E. Olfactory hallucinations elicited by electrical stimulation via subdural electrodes: effects of direct stimulation of olfactory bulb and tract. Epilepsy Behav. 2012; 24:264–8. [PubMed: 22554977]

Marshall L, Helgadóttir H, Mölle M, Born J. Boosting slow oscillations during sleep potentiates memory. Nature. 2006; 444:610–3. [PubMed: 17086200]

Matsuzaki N, Schwarzlose RF, Nishida M, Ofen N, Asano E. Upright face-preferential high-gamma responses in lower-order visual areas: evidence from intracranial recordings in children. Neuroimage. 2015; 109:249–59. [PubMed: 25579446]

Melani F, Zelmann R, Mari F, Gotman J. Continuous High Frequency Activity: a peculiar SEEG pattern related to specific brain regions. Clin Neurophysiol. 2013; 124:1507–16. [PubMed: 23768436]

Miyakoshi M, Delorme A, Mullen T, Kojima K, Makeig S, Asano E. Automated detection of cross-frequency coupling in the electrocorticogram for clinical inspection. Conf Proc IEEE Eng Med Biol Soc. 2013; 2013:3282–5.10.1109/EMBC.2013.6610242 [PubMed: 24110429]

Moeller F, Siebner HR, Wolff S, Muhle H, Granert O, Jansen O, Stephani U, Siniatchkin M. Simultaneous EEG-fMRI in drug-naive children with newly diagnosed absence epilepsy. Epilepsia. 2008; 49:1510–9. [PubMed: 18435752]

Mouthaan BE, van 't Klooster MA, Keizer D, Hebbink GJ, Leijten FS, Ferrier CH, van Putten MJ, Zijlmans M, Huiskamp GJ. Single Pulse Electrical Stimulation to identify epileptogenic cortex: Clinical information obtained from early evoked responses. Clin Neurophysiol. 201510.1016/j.clinph.2015.07.031

Nagasawa T, Juhász C, Rothermel R, Hoechstetter K, Sood S, Asano E. Spontaneous and visually driven high-frequency oscillations in the occipital cortex: intracranial recording in epileptic patients. Hum Brain Mapp. 2012; 33:569–83. [PubMed: 21432945]

Nariai H, Nagasawa T, Juhász C, Sood S, Chugani HT, Asano E. Statistical mapping of ictal high-frequency oscillations in epileptic spasms. Epilepsia. 2011; 52:63–74. [PubMed: 21087245]

Nayak D, Valentín A, Selway RP, Alarcón G. Can single pulse electrical stimulation provoke responses similar to spontaneous interictal epileptiform discharges? Clin Neurophysiol. 2014; 125:1306–11. [PubMed: 24424009]

Okanari K, Baba S, Otsubo H, Widjaja E, Sakuma S, Go CY, Jones KC, Nishioka K, Oba S, Matsui T, Ueno M, Ukitsu S, Rutka JT, Drake JM, Donner EJ, Weiss SK, Snead OC 3rd, Ochi A. Rapid eye movement sleep reveals epileptogenic spikes for resective surgery in children with generalized interictal discharges. Epilepsia. 2015; 56:1445–53. [PubMed: 26174651]

Onton J, Makeig S. Information-based modeling of event-related brain dynamics. Prog Brain Res. 2006; 159:99–120. [PubMed: 17071226]

Otsubo H, Ochi A, Imai K, Akiyama T, Fujimoto A, Go C, Dirks P, Donner EJ. High-frequency oscillations of ictal muscle activity and epileptogenic discharges on intracranial EEG in a temporal lobe epilepsy patient. Clin Neurophysiol. 2008; 119:862–8. [PubMed: 18289931]

Pieters TA, Conner CR, Tandon N. Recursive grid partitioning on a cortical surface model: an optimized technique for the localization of implanted subdural electrodes. J Neurosurg. 2013; 118:1086–97. [PubMed: 23495883]

Rosenow F, Lüders H. Presurgical evaluation of epilepsy. Brain. 2001; 124:1683–700. [PubMed: 11522572]

Sakuraba R, Iwasaki M, Okumura E, Jin K, Kakisaka Y, Kato K, Tominaga T, Nakasato N. High frequency oscillations are less frequent but more specific to epileptogenicity during rapid eye movement sleep. Clin Neurophysiol. 201510.1016/j.clinph.2015.05.019

Sanchez-Vives MV, McCormick DA. Cellular and network mechanisms of rhythmic recurrent activity in neocortex. Nat Neurosci. 2000; 3:1027–34. [PubMed: 11017176]

Sasaki Y, Nanez JE, Watanabe T. Advances in visual perceptual learning and plasticity. Nat Rev Neurosci. 2010; 11:53–60. [PubMed: 19953104]

Schroeder CE, Lakatos P. Low-frequency neuronal oscillations as instruments of sensory selection. Trends Neurosci. 2009; 32:9–18. [PubMed: 19012975]

Staba RJ, Wilson CL, Bragin A, Fried I, Engel J Jr. Quantitative analysis of high-frequency oscillations (80–500 Hz) recorded in human epileptic hippocampus and entorhinal cortex. J Neurophysiol. 2002; 88:1743–52. [PubMed: 12364503]

Steriade M, Nuñez A, Amzica F. A novel slow (< 1 Hz) oscillation of neocortical neurons in vivo: depolarizing and hyperpolarizing components. J Neurosci. 1993; 13:3252–65. [PubMed: 8340806]

Steriade M, Timofeev I. Neuronal plasticity in thalamocortical networks during sleep and waking oscillations. Neuron. 2003; 37:563–76. [PubMed: 12597855]

Usui N, Terada K, Baba K, Matsuda K, Usui K, Tottori T, Mihara T, Inoue Y. Significance of Very-High-Frequency Oscillations (Over 1,000Hz) in Epilepsy. Ann Neurol. 2015; 78:295–302. [PubMed: 25974128]

van't Klooster MA, Zijlmans M, Leijten FS, Ferrier CH, van Putten MJ, Huiskamp GJ. Time-frequency analysis of single pulse electrical stimulation to assist delineation of epileptogenic cortex. Brain. 2011; 134:2855–66. [PubMed: 21900209]

van't Klooster MA, van Klink NE, Leijten FS, Zelmann R, Gebbink TA, Gosselaar PH, Braun KP, Huiskamp GJ, Zijlmans M. Residual fast ripples in the intraoperative corticogram predict epilepsy surgery outcome. Neurology. 2015; 85:120–8. [PubMed: 26070338]

Voytek B, Canolty RT, Shestyuk A, Crone NE, Parvizi J, Knight RT. Shifts in gamma phase-amplitude coupling frequency from theta to alpha over posterior cortex during visual tasks. Front Hum Neurosci. 2010; 4:191. [PubMed: 21060716]

Wang S, Wang IZ, Bulacio JC, Mosher JC, Gonzalez-Martinez J, Alexopoulos AV, Najm IM, So NK. Ripple classification helps to localize the seizure-onset zone in neocortical epilepsy. Epilepsia. 2013; 54:370–6. [PubMed: 23106394]

Weiss SA, Banks GP, McKhann GM Jr, Goodman RR, Emerson RG, Trevelyan AJ, Schevon CA. Ictal high frequency oscillations distinguish two types of seizure territories in humans. Brain. 2013; 136:3796–808. [PubMed: 24176977]

Widdess-Walsh P, Jeha L, Nair D, Kotagal P, Bingaman W, Najm I. Subdural electrode analysis in focal cortical dysplasia: predictors of surgical outcome. Neurology. 2007; 69:660–7. [PubMed: 17698787]

Worrell GA, Gardner AB, Stead SM, Hu S, Goerss S, Cascino GJ, Meyer FB, Marsh R, Litt B. High-frequency oscillations in human temporal lobe: simultaneous microwire and clinical macroelectrode recordings. Brain. 2008; 131:928–37. [PubMed: 18263625]

Wu JY, Sankar R, Lerner JT, Matsumoto JH, Vinters HV, Mathern GW. Removing interictal fast ripples on electrocorticography linked with seizure freedom in children. Neurology. 2010; 75:1686–94. [PubMed: 20926787]

Zijlmans M, Jacobs J, Zelmann R, Dubeau F, Gotman J. High-frequency oscillations mirror disease activity in patients with epilepsy. Neurology. 2009; 72:979–86. [PubMed: 19289737]

Zijlmans M, Jiruska P, Zelmann R, Leijten FS, Jefferys JG, Gotman J. High-frequency oscillations as a new biomarker in epilepsy. Ann Neurol. 2012; 71:169–78. [PubMed: 22367988]

HIGHLIGHTS

1. Interictal HFOs were noted in seizure-onset and sensorimotor-visual sites during sleep.
2. Epileptogenic HFOs may be more preferentially coupled with slow waves of 3–4 Hz.
3. Physiologic HFOs may be more preferentially coupled with slow waves of 0.5–1 Hz.

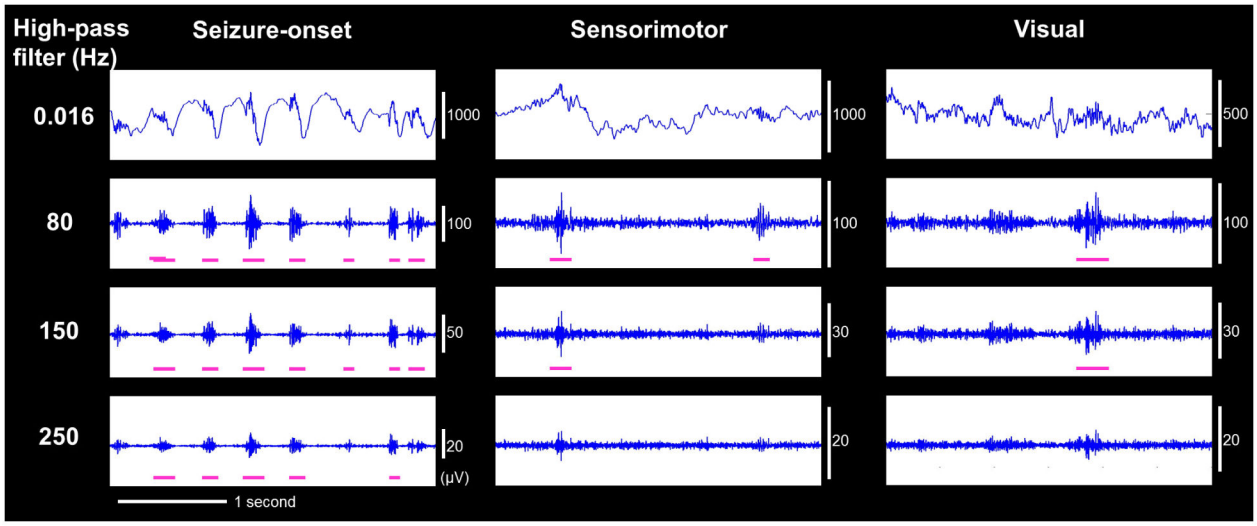

Figure 1. ECoG during interictal state in patient #1

Interictal ECoG traces at (A) seizure-onset, (B) nonepileptic sensorimotor, and (C) nonepileptic visual sites are shown with high-pass filter at 0.016, 80, 150, and 250 Hz. High-frequency oscillations (HFOs) were accompanied by a steep slow wave at the seizure-onset site but a dull slow wave at the nonepileptic sensorimotor and visual sites.

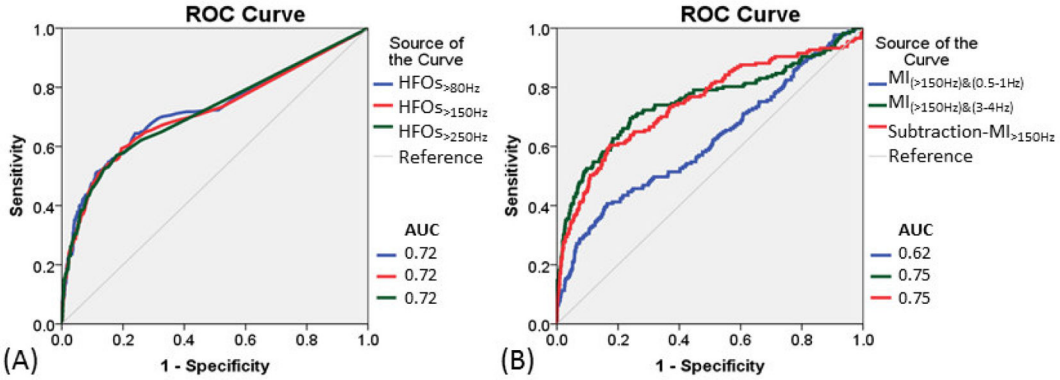

Figure 2. Seizure-onset localization by HFOs and modulation index (MI) measures

(A) Receiver-operating characteristics (ROC) curves for localization of seizure-onset sites using rates of $HFOs_{>80Hz}$ (blue line), $HFOs_{>150Hz}$ (red line), and $HFOs_{>250Hz}$ (green line). (B) ROC curves for localization of seizure-onset sites using $MI_{(>150Hz)\&(0.5–1Hz)}$ (blue line), $MI_{(>150Hz)\&(3–4Hz)}$, (green line), and subtraction-$MI_{>150Hz}$ (defined as subtraction of $MI_{(>150Hz)\&(0.5–1Hz)}$ from $MI_{(>150Hz)\&(3–4Hz)}$ [red line]).

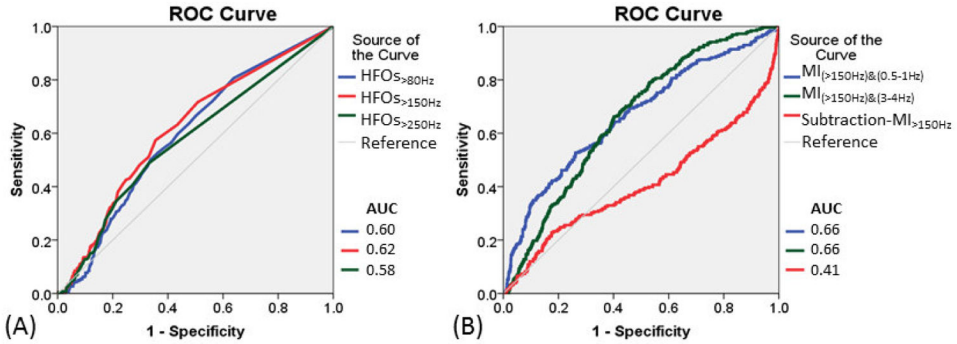

Figure 3. Undesirable detection of nonepileptic sensorimotor-visual sites by HFOs and modulation index (MI) measures

(A) Receiver-operating characteristics (ROC) curves for assessment of undesirable detection of nonepileptic sensorimotor-visual sites using rates of $HFOs_{>80Hz}$ (blue line), $HFOs_{>150Hz}$ (red line), and $HFOs_{>250Hz}$ (green line). (B) ROC curves for assessment of undesirable detection of nonepileptic sensorimotor-visual sites using $MI_{(>150Hz)\&(0.5–1Hz)}$ (blue line), $MI_{(>150Hz)\&(3–4Hz)}$ (green line), and subtraction-$MI_{>150Hz}$ [defined as subtraction of $MI_{(>150Hz)\&(0.5–1Hz)}$ from $MI_{(>150Hz)\&(3–4Hz)}$] (red line). Increase in subtraction-$MI_{>150Hz}$ reduced undesirable detection of nonepileptic sensorimotor-visual sites.

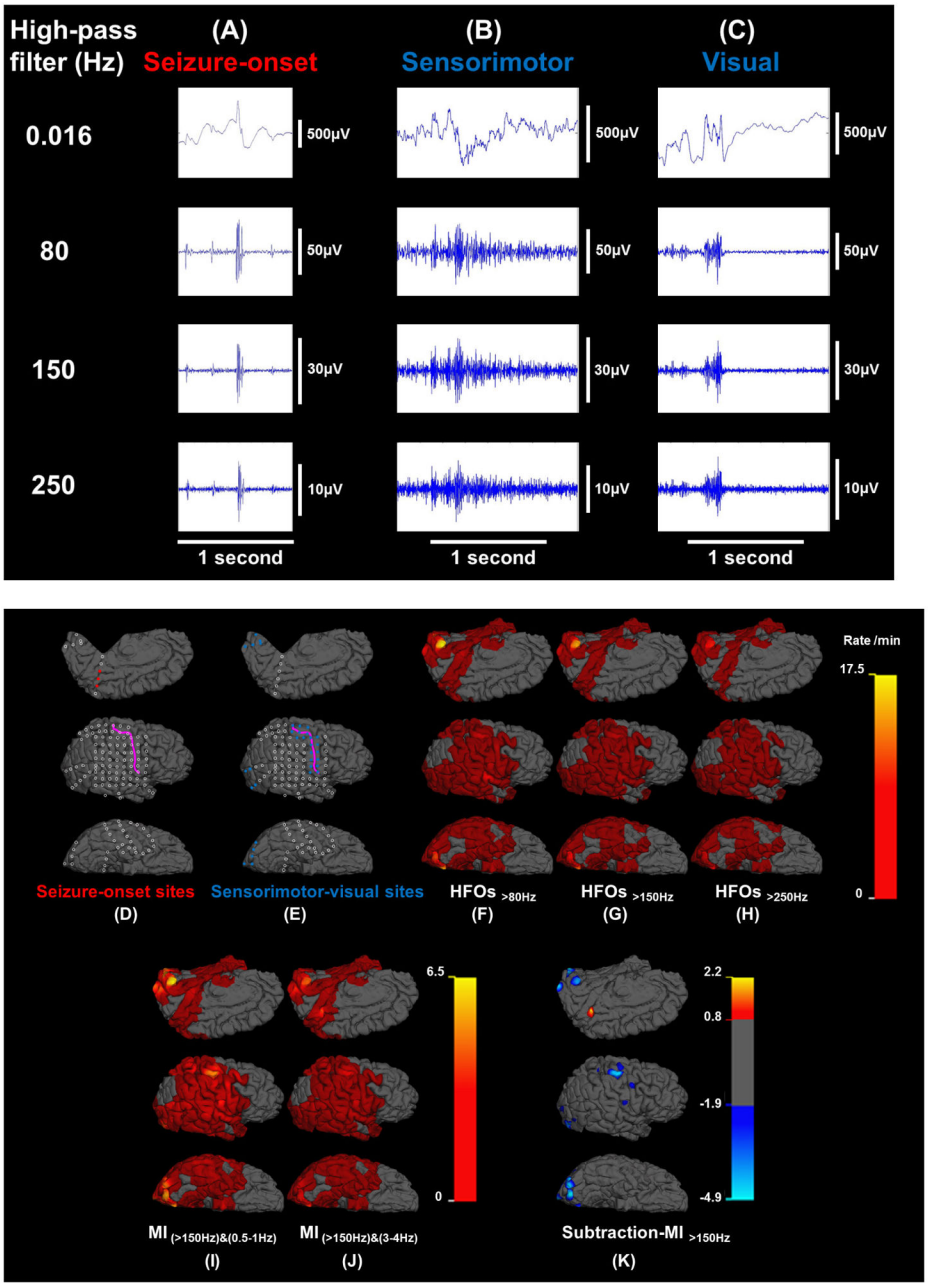

Figure 4. Spatial profiles of the rates of high-frequency oscillations (HFOs) and modulation index (MI) in patient #11

HFO events at (A) seizure-onset, (B) sensorimotor, and (C) visual sites. (D) Seizure-onset sites: red circles. (E) Sensorimotor-visual sites: blue circles. (F) Rate of $HFOs_{>80Hz}$ (event/min). (G) Rate of $HFOs_{>150Hz}$. (H) Rate of $HFOs_{>250Hz}$. (I) $MI_{(>150Hz)\&(0.5–1Hz)}$. (J) $MI_{(>150Hz)\&(3–4Hz)}$. (K) Subtraction-$MI_{>150Hz}$ co-registered to MRI (SMICOM). Subtraction-$MI_{>150Hz}$ was defined as subtraction of $MI_{(>150Hz)\&(0.5–1Hz)}$ from $MI_{(>150Hz)\&(3–4Hz)}$. The highest value was noted in the seizure onset site, whereas nonepileptic sensorimotor-visual sites were associated with negative values.

Table 1

Patient profile.

Patient number	Age	Gender	History of epileptic spasms	Sampled hemisphere	Seizure onset zone	Surgical resection	MRI	Pathology	ILAE seizure outcome	Follow-up period (month)
1 *	7.9	M	Yes	Right	TPO	Resection of TPO and insular cortex	Non-lesional	Dysplasia	4 *	3
2	8.3	M	No	Right	TO	Resection of TO	Dysplasia or tumor	DNET associated with dysplasia	1	24
3	11.5	F	No	Right	P	Resection of P	Non-lesional	Gliosis	1	15
4	11.9	F	Yes	Left	TPO	Resection of TPO	Dysplasia	Dysplasia	1	22
5	12.0	F	Yes	Left	FP	Resection of FP	Cortical tuber	Cortical tuber	1	24
6	12.5	F	No	Left	P	Resection of P	Calcification	Oligodendroglioma	1	14
7	12.9	F	No	Left	T	Resection of T	Non-lesional	Gliosis	1	20
8	13.7	F	No	Left	T	Resection of T	Non-lesional	Gliosis	4	23
9	13.9	F	No	Right	T	Resection of T	Non-lesional	Gliosis	3	19
10	14.5	F	No	Left	T	Resection of T	Non-lesional	Gliosis and medial-temporal sclerosis	1	15
11	14.7	F	No	Right	P	Resection of P	Non-lesional	Dysplasia	3	21
12	17.8	M	No	Left	F	Resection of F	Non-lesional	Dysplasia	1	13
13	18.8	F	Yes	Right	TFP	Subtotal Hemispherectomy	Non-lesional	Dysplasia	1	17

F: frontal. T: temporal. P: parietal. O: occipital. Subtotal hemispherectomy: multilobar resection involving all four lobes but the pre- and post-central gyri preserved.

* Patient #1 enjoyed cessation of habitual epileptic spasms for eight months following the first surgery consisting of temporal-occipital-parietal resection with the post-central gyrus preserved, but focal seizures involving the face and throat newly took place afterwards. This patient has been free from both spasms and focal seizures for three months following the second surgery consisting of resection of the parietal operculum and insular cortex not originally sampled in the first surgery.

Table 2

ROC analysis for assessment of performance of HFOs and MI measures for localization of seizure-onset sites.

Predictor	AUC	95%CI Lower	95%CI Upper	P-value	Cut-off threshold for sensitivity of 0.5 *	Specificity
Rate of $HFOs_{>80Hz}$	0.72	0.68	0.77	<0.001	4.90	0.89
Rate of $HFOs_{>150Hz}$	0.72	0.67	0.76	<0.001	2.65	0.88
Rate of $HFOs_{>250Hz}$	0.72	0.67	0.76	<0.001	0.65	0.88
$MI_{(>80Hz)\&(0.5–1Hz)}$	0.65	0.60	0.70	<0.001	4.68	0.76
$MI_{(>150Hz)\&(0.5–1Hz)}$	0.62	0.57	0.67	<0.001	0.73	0.64
$MI_{(>250Hz)\&(0.5–1Hz)}$	0.58	0.53	0.63	<0.001	0.16	0.55
$MI_{(>80Hz)\&(3–4Hz)}$	**0.77**	0.73	0.82	<0.001	7.06	0.94
$MI_{(>150Hz)\&(3–4Hz)}$	0.75	0.71	0.80	<0.001	1.38	0.91
$MI_{(>250Hz)\&(3–4Hz)}$	0.74	0.69	0.79	<0.001	0.27	0.88
Subtraction-$MI_{>80Hz}$	0.71	0.66	0.76	<0.001	0.90	0.88
Subtraction-$MI_{>150Hz}$	0.75	0.70	0.79	<0.001	0.31	0.89
Subtraction-$MI_{>250Hz}$	0.75	0.71	0.80	<0.001	0.08	0.91

The results of receiver-operating characteristics (ROC) analysis are summarized. An area under the curve (AUC) larger than 0.5 reflects a given predictor measure was larger at seizure-onset sites compared to at non-seizure-onset sites. A larger AUC indicates a greater seizure-onset localization performance. A 95% confidence interval (95%CI) of the AUC is provided for each predictor variable.

*Cut-off threshold indicates the threshold of a given predictor variable resulting in a sensitivity of 0.5 for localization of seizure-onset sites. For example, electrode sites showing an occurrence rate of $HFOs_{>150Hz}$ above 2.65/min localized seizure-onset sites with a sensitivity of 0.50 and specificity of 0.88. For interested readers, we have provided Supplementary Table S3 showing the mean sensitivity and specificity across 13 patients when the aforementioned cut-off threshold was applied to each individual patient. This ancillary data also suggest that the performance of seizure-onset localization by $MI_{(HFOs)\&(3–4Hz)}$ and subtraction-MIHFOs was at least comparable to that by rates of HFOs.

Table 3

Logistic regression analysis for assessment of performance of HFOs and MI measures for localization of seizure-onset sites.

Predictor	P-value	Odds ratio	95%CI Lower	95%CI Upper
Rate of $HFOs_{>80Hz}$	<0.001	1.15	1.12	1.18
Rate of $HFOs_{>150Hz}$	<0.001	1.17	1.14	1.21
Rate of $HFOs_{>250Hz}$	<0.001	1.33	1.25	1.41
$MI_{(>80Hz)\&(0.5–1Hz)}$	<0.001	1.09	1.07	1.12
$MI_{(>150Hz)\&(0.5–1Hz)}$	<0.001	1.48	1.33	1.64
$MI_{(>250Hz)\&(0.5–1Hz)}$	<0.001	4.48	2.76	7.27
$MI_{(>80Hz)\&(3–4Hz)}$	<0.001	1.21	1.17	1.25
$MI_{(>150Hz)\&(3–4Hz)}$	<0.001	2.24	1.94	2.57
$MI_{(>250Hz)\&(3–4Hz)}$	<0.001	30.75	16.48	57.39
Subtraction-$MI_{>80Hz}$	<0.001	1.17	1.12	1.23
Subtraction-$MI_{>150Hz}$	<0.001	2.29	1.90	2.75
Subtraction-$MI_{>250Hz}$	<0.001	**40.55**	17.89	91.90

The results of logistic regression analysis are summarized. All tested predictors were found to be useful to localize seizure onset sites. Each increase of 1 subtraction-$MI_{>150Hz}$, for example, increased the odds of a given site classified as seizure onset by 2.29 times. The excellent odds ratio of subtraction-$MI_{>250Hz}$ is at least partly attributed to the smaller range of this variable (Supplementary Table S2).

Table 4

ROC analysis for assessment of performance of HFOs and MI measures for localization of nonepileptic sensorimotor-visual sites.

Predictor	AUC	95%CI Lower	95%CI Upper	P-value	Cut-off threshold for sensitivity of 0.5 *	Specificity
Rate of $HFOs_{>80Hz}$	0.60	0.56	0.63	<0.001	0.85	0.66
Rate of $HFOs_{>150Hz}$	0.62	0.58	0.65	<0.001	0.35	0.67
Rate of $HFOs_{>250Hz}$	0.58	0.54	0.62	<0.001	0.05	0.67
$MI_{(>80Hz)\&(0.5–1Hz)}$	0.60	0.56	0.64	<0.001	3.31	0.62
$MI_{(>150Hz)\&(0.5–1Hz)}$	0.66	0.63	0.70	<0.001	0.86	0.75
$MI_{(>250Hz)\&(0.5–1Hz)}$	0.66	0.62	0.70	<0.001	0.21	0.71
$MI_{(>80Hz)\&(3–4Hz)}$	0.59	0.55	0.62	<0.001	1.93	0.63
$MI_{(>150Hz)\&(3–4Hz)}$	0.66	0.63	0.69	<0.001	0.52	0.70
$MI_{(>250Hz)\&(3–4Hz)}$	0.66	0.62	0.69	<0.001	0.13	0.70
Subtraction-$MI_{>80Hz}$	0.42	0.38	0.46	<0.001	−1.41	0.35
Subtraction-$MI_{>150Hz}$	**0.41**	0.37	0.45	<0.001	−0.28	0.34
Subtraction-$MI_{>250Hz}$	**0.41**	0.37	0.45	<0.001	−0.08	0.33

An area under the curve (AUC) larger than 0.5 reflects a given predictor measure was larger at nonepileptic sensorimotor-visual sites compared to at non-sensorimotor-visual sites. Thus, a larger AUC indicates that increase in a given predictor variable undesirably localized nonepileptic sensorimotor-visual sites. Conversely, a smaller AUC indicates that increase in a given predictor variable can avoid such undesirable detection of nonepileptic sensorimotor-visual sites.

* Cut-off threshold indicates the threshold of a given predictor variable resulting in a sensitivity of 0.5 for undesirable localization of nonepileptic sensorimotor-visual sites. For example, electrode sites showing a rate of $HFOs_{>150Hz}$ above 0.35/min undesirably localized nonepileptic sensorimotor-visual sites with a sensitivity of 0.50 and specificity of 0.67. For interested readers, we have provided Supplementary Table S4 showing the mean sensitivity and specificity across 13 patients when the aforementioned cut-off threshold was applied to each individual patient.

Table 5

Logistic regression analysis for assessment of performance of HFOs and MI measures for localization of nonepileptic sensorimotor-visual sites.

Predictor	P-value	Odds ratio	95%CI Lower	95%CI Upper
Rate of $HFOs_{>80Hz}$	0.82	1.00	0.97	1.02
Rate of $HFOs_{>150Hz}$	0.21	1.02	0.99	1.05
Rate of $HFOs_{>250Hz}$	0.90	1.00	0.94	1.05
$MI_{(>80Hz)\&(0.5–1Hz)}$	0.37	1.01	0.99	1.03
$MI_{(>150Hz)\&(0.5–1Hz)}$	<0.001	1.27	1.16	1.40
$MI_{(>250Hz)\&(0.5–1Hz)}$	<0.001	6.28	3.73	10.55
$MI_{(>80Hz)\&(3–4Hz)}$	0.097	0.97	0.95	1.00
$MI_{(>150Hz)\&(3–4Hz)}$	0.085	1.07	0.99	1.15
$MI_{(>250Hz)\&(3–4Hz)}$	0.002	1.84	1.26	2.70
Subtraction-$MI_{>80Hz}$	<0.001	0.94	0.92	0.97
Subtraction-$MI_{>150Hz}$	<0.001	0.66	0.56	0.77
Subtraction-$MI_{>250Hz}$	<0.001	**0.15**	0.07	0.30

Odds ratio greater than 1 indicates that each unit increase of a given predictor increased the odds of a given site classified as nonepileptic sensorimotor-visual area. Conversely, increased subtraction-MI_{HFOs} was associated with decreased risk of undesirable detection of sensorimotor-visual sites.